



Published in final edited form as:

*Eur J Pharm Biopharm.* 2011 May ; 78(1): 107–116. doi:10.1016/j.ejpb.2010.12.017.

## Relationship between the size of nanoparticles and their adjuvant activity: Data from a study with an improved experimental design

Xinran Li, Brian R. Sloat, Nijaporn Yanasarn, and Zhengrong Cui\*

The University of Texas at Austin, Pharmaceutics Division, College of Pharmacy, Austin, TX 78712

### Abstract

There is a growing interest in identifying the relationship between the size of nanoparticles and their adjuvant activity, but the results from recent studies remain controversial. To address the controversy, it was thought that one should pay attention to the nanoparticle formulations to make sure that the antigen-loaded nanoparticles to be compared are not only different in particle size, but more importantly, as identical to each other as possible in all other formulation properties. In the present study, using ovalbumin (OVA) as a model antigen conjugated onto nanoparticles engineered from lecithin/glyceryl monostearate-in-water emulsions, we prepared OVA-nanoparticles of 230 nm and 708 nm. Before evaluating the immune responses induced by them in a mouse model, we made sure that: i) the sizes of the two OVA-nanoparticles did not extensively overlap, ii) the nanoparticles have similar zeta potentials and comparable antigen-loading, and iii) the nanoparticles did not aggregate when suspended in simulated biological media. We then showed that when subcutaneously injected into mice, the 230 nm OVA-conjugated nanoparticles induced stronger OVA-specific antibody and cellular immune responses than the 708 nm OVA-nanoparticles. Future studies attempting to correlate the size of nanoparticles and their adjuvant activities need to consider formulation parameters to ensure that the particles are different only in size and are stable before and after injection.

### Keywords

Immune responses; tumor treatment; particle uptake; particle trafficking

### 1. Introduction

Many particles of nanometer or micrometer scales as antigen carriers have vaccine adjuvant activity [1–3]. However, data from studies that attempted to correlate the size of the particles and their adjuvant activity have been controversial [4–11]. Some researchers showed that larger particles were more potent than smaller particles [7,10], while others showed the exact opposite [8]. There were also data showing that the size of particles did not affect the

© 2010 Elsevier B.V. All rights reserved.

\*Correspondence to: Zhengrong Cui, Ph.D., The University of Texas at Austin, Dell Pediatric Research Institute, 1400 Barbara Jordan Boulevard, Austin, Texas 78723, Tel: (512) 495-4758, Fax: (512) 471-7474, zhengrong.cui@austin.utexas.edu.

**Publisher's Disclaimer:** This is a PDF file of an unedited manuscript that has been accepted for publication. As a service to our customers we are providing this early version of the manuscript. The manuscript will undergo copyediting, typesetting, and review of the resulting proof before it is published in its final citable form. Please note that during the production process errors may be discovered which could affect the content, and all legal disclaimers that apply to the journal pertain.

resultant immune responses [11], and data from some studies suggested that there may be an ideal particle size with the most potent vaccine adjuvant activity [6,9]. Interestingly, it also becomes evident that the size of the particles influences the type of immune responses induced as well [12–14], but it again remains controversial as to whether small or large particles favor T helper type 1 (Th1) vs. Th2 or antibody vs. cellular immune responses [10,14–15].

In a previous article, it was pointed out that factors that may have contributed to the controversial findings include: i) materials used to prepare the particles, ii) nature of antigens used, iii) methods of antigen loading, and (iv) routes of administration [16]. When the same antigen was loaded onto particles of different size prepared with the same materials and then administered via the same route into the same strain of animals, it was thought that one should make sure that firstly, except the difference in size, the particles to be compared are as close to identical as possible to each other. For example, the zeta potentials of different particles to be compared should not be different, and not only the same amount of antigens, but also the same amount of particulates (excluding the amount of antigens) should be injected. The zeta potential and amount of particles injected may affect the resultant immune responses, but rarely had they been reported. Secondly, the size of the particles should be that after the loading of antigens, not that before antigen loading [6]. This is particularly important if the antigens are covalently conjugated onto the particles or bound on the particles by electrostatic interactions. For example, it was shown that conjugation of OVA onto 40–50 nm-polystyrene nanoparticles resulted in OVA-polystyrene particles of 230 nm [6,9]. Similarly, when anionic nanoparticles of  $78 \pm 11$  nm prepared with emulsifying wax and sodium dodecyl sulfate were coated with cationized  $\beta$ -galactosidase protein, the resultant particle size became 208–354 nm [17]. Thirdly, if the antigen-loaded particles are unstable or aggregate during storage, their size immediately before dosing to animals should be measured [16]. Fourthly, the final antigen-loaded particles should not aggregate after being injected into animals, which may be predicted by monitoring whether the particles aggregate in simulated biological media [16]. Finally, the particle size should be as uniform as possible and narrowly distributed, and the sizes of the particles to be compared should not extensively overlap. It is possible that the wide particle size range used in some previous studies had contributed, to a certain extent, to the controversial results. For example, in a previous study, bilosome particles of 400–2500 nm and 60–350 nm were compared [15]. It is likely that in the 400–2500 nm range, the 400 nm particles and the 2500 nm particles had different adjuvant activities because data from another study showed that antigen-loaded particles of 200–600 nm and 2000–8000 nm induced different immune responses [10].

Previously, Sloat *et al.* (2010) reported the engineering of nanoparticles with diameters ranging from 200 to 700 nm from lecithin/glyceryl monostearate-in-water emulsions [3]. It was shown that antigens conjugated onto the surface of nanoparticles of around 200 nm induced a strong and functional specific antibody response when subcutaneously injected into mice [3]. In the present study, we decided to use OVA as a model antigen and conjugated it onto the surface of nanoparticles to generate OVA-nanoparticles smaller or larger than 500 nm and to evaluate the immune responses induced by them in a mouse model. Nanoparticles smaller and larger than 500 nm were chosen because data from studies investigating particle uptake and antigen capture showed that particles of 500 nm or smaller were optimal for uptake by antigen-presenting cells (APCs) such as dendritic cells (DCs) and macrophages [10,18]. It was also shown that when injected subcutaneously into the hind leg footpads of mice, small nanoparticles (20–200 nm) freely drained to local draining popliteal lymph nodes, whereas large particles (500 nm–2  $\mu$ m) required DCs for transport from the injection site to the lymph nodes [19]. Based on those findings, we hypothesized that nanoparticles smaller than 500 nm and large than 500 nm would have different adjuvant

activities. After making sure that the small and large OVA-nanoparticles did not extensively overlap in particle size, had similar zeta potentials, contained similar amount of OVA protein and nanoparticles, and did not aggregate in simulated biological media, we showed that the small 230 nm OVA-nanoparticles induced stronger antibody and cellular immune responses than the large 700 nm OVA-nanoparticles. This study may be used as a template in designing future experiments attempting to define the relationship between the size of nanoparticles and their adjuvant activities.

## 2. Materials and Methods

### 2.1. Materials

OVA, fluorescein-5(6)-isothiocyanate (FITC), 2-iminothiolane (Traut's reagent), 3,3',5,5'-tetramethylbenzidine (TMB) solution, sodium bicarbonate, sodium carbonate, Tween 20, and phosphate-buffered saline (PBS), 5-(and-6-)carboxylfluorescein diacetate, succinimidyl ester (CFSE) were from Sigma-Aldrich (St. Louis, MO). Lecithin (soy, refined) was from Alfa Aesar (Ward Hill, MA). Glyceryl monostearate (GMS) was from Gattefosse Corp. (Paramus, NJ). 1, 2-dipalmitoyl-*sn*-glycero-3-phosphoethanolamine-N-[4-(*p*-maleimidophyl) butyramide] (DPPE-maleimide) and 1,2-dioleoyl-*sn*-glycero-3-phosphoethanolamine-N-carboxyfluorescein (DOPE-fluorescein) were from Avanti Polar Lipids (Alabaster, AL). Goat anti-mouse immunoglobulins (IgG, IgG1, and IgG2a) were from Southern Biotechnology Associates, Inc. (Birmingham, AL). Fluorescence-labeled anti-I-A[b], anti-H-2kb, and anti-CD80 antibodies were from BD Pharmingen (San Diego, CA). Carbon-coated 400-mesh grids were from Electron Microscopy Sciences (Hatfield, PA). Vectashield mounting medium with DAPI (4',6-diamidino-2-phenylindole) was from Vector Laboratories, Inc. (Burlingame, CA).

### 2.2. Mice and cell lines

Female C57BL/6 mice, 6–7 weeks of age, were from Simonsen laboratories (Gilroy, CA) or Charles River Laboratories (Wilmington, MA). The OVA-expressing B16-OVA cell line was generously provided by Dr. Edith M. Lord and Dr. John Frelinger (University of Rochester Medical Center, Rochester, NY) [20]. Mouse J774A.1 macrophage cells (# TIB-67™) were from ATCC (Manassas, VA). DC2.4 cells were created by Dr. Kenneth L. Rock (University of Massachusetts Medical School, Worcester, MA) [21]. Culture medium, fetal bovine serum (FBS), and antibiotics were from Invitrogen (Carlsbad, CA). B16-OVA cells were cultured in RPMI 1640 medium supplemented with 5% FBS and 400 µg/ml of G418 (Sigma). DC2.4 cells (a mouse DC line) and J774A.1 cells (a mouse macrophage line) were grown in RPMI 1640 medium and DMEM medium, respectively. The culture media were supplemented with 10% FBS, 100 U/ml of penicillin and 100 µg/ml of streptomycin.

### 2.3. Preparation of nanoparticles

Nanoparticles were prepared as previously described [3,22]. Briefly, soy lecithin (3.5 mg) and GMS (0.5 mg) were weighed into a 7-ml glass vial. One milliliter of de-ionized and filtered (0.22 µm) water was added into the vial, followed by heating on a hot plate to 70–75°C with stirring and brief intermittent periods of sonication (Ultrasonic Cleaner Model 150T, VWR International, West Chester, PA). Once a homogenous milky slurry was formed, Tween 20 was added in a step-wise manner to the slurry to a final concentration of 1% (v/v) or 0.4% to form emulsions. The resultant emulsions were allowed to stay at room temperature while stirring to form nanoparticles (small with 1% of Tween 20, large with 0.4% of Tween 20). The endotoxin level in the nanoparticle preparations was estimated to be 0.18–0.57 EU/ml using a ToxinSensor™ Chromogenic LAL Endotoxin Assay Kit from GenScript (Piscataway, NJ). The size of the nanoparticles was determined using a Beckman-Coulter Delsa Nano C Particle Sizer (Brea, CA) or a Malvern Zetasizer Nano ZS

(Worcestershire, United Kingdom). To prepare maleimide-nanoparticles, DPPE-maleimide, which has a reactive maleimide group, was included in the lipid mixture (5%, w/w) [3].

#### 2.4. Conjugation of protein antigen onto the nanoparticles

The conjugation of OVA as an antigen onto the nanoparticles was completed as previously described [3,22]. Prior to conjugation, OVA was thiolated using Traut's Reagent. OVA was diluted into PBS (0.1 M with 3.0 mM EDTA, pH 8.0), followed by the addition of Traut's reagent (20 × molar excess) and a 60 min incubation at room temperature. Thiolated OVA was desalted using a PD10 column (GE Healthcare, Piscataway, NJ). To react the thiolated OVA with nanoparticles, 1 ml of freshly prepared maleimide-nanoparticles were mixed with the thiolated OVA (1 mg) in PBS (0.1 M, pH 7.4) and stirred under N<sub>2</sub> gas for 12–14 h at room temperature. Un-conjugated OVA was removed by repeated ultracentrifugation (600,000 × g) and washing (with PBS) for 3 times. The amount of OVA conjugated onto the nanoparticles was estimated as previously described using FITC-labeled OVA [3]. The OVA-nanoparticles (after the final wash) were freeze-dried for 48 h using a Labconco FreeZone 4.5 Plus freeze-dryer (Kansas City, MO), and the weight of the final dried powder was measured. The conjugation efficiency was reported as the amount of OVA (μg) conjugated onto 1 mg of OVA-free nanoparticles. The size and zeta potential of the OVA-conjugated nanoparticles diluted in water were measured using a Malvern Zetasizer Nano ZS.

#### 2.5. Stability of nanoparticles in simulated biological media

To evaluate the stability of nanoparticles in simulated biological media, OVA-nanoparticles were diluted into normal saline or normal saline with 10% (v/v) FBS [3]. The size of the nanoparticles was measured immediately after the dilution and then after 30 min incubation at 37°C.

#### 2.6. Transmission electron microscopy (TEM)

The size and morphology of the OVA-nanoparticles were observed using an FEI Tecnai Transmission Electron Microscope in the Institute for Cellular and Molecular Biology Microscopy and Imaging Facility at The University of Texas at Austin [3].

#### 2.7. Immunization studies

All animal studies were carried out following National Institutes of Health guidelines for animal care and use. Animal protocol was approved by the Institutional Animal Care and Use Committee at The University of Texas at Austin. Female C57BL/6 mice (18–20 g) were immunized once a week for three consecutive weeks by subcutaneous injection of OVA-conjugated nanoparticles (OVA-NPs, small, large, or their mixture (OVA dose, 1:1, w/w)), OVA adjuvanted with incomplete Freund's adjuvant (IFA, Sigma) (OVA/IFA), or OVA physically mixed with nanoparticles (OVA+NPs). As a negative control, mice were injected with sterile PBS or OVA in PBS. Twenty one days after the first immunization, mice were bled for antibody assay. The dose of OVA in these studies was 50 μg per mouse.

In tumor treatment studies, B16-OVA cells (50,000/mouse) were subcutaneously injected in the right flank of C57BL/6 mice. Four or 7 days later, mice were injected subcutaneously with OVA-NPs (large, small, or their mixture), OVA adjuvanted with IFA, or OVA in PBS. Mice in the negative control group were injected with sterile PBS. The injection was repeated once a week for two more weeks. The dose of the OVA in the treatment studies was 75 μg per mouse. Tumor size was measured using a caliper and reported based on the following equation: Tumor volume (mm<sup>3</sup>) = 1/2 [length × (width)<sup>2</sup>]. The time it took for tumors to reach 15 mm in diameter was recorded to construct survival curves.

## 2.8. Enzyme-linked immunosorbent assay (ELISA)

ELISA was completed as previously described [3,22]. The antibody titers were determined by considering any OD450 absorbance value higher than the mean  $\pm 2 \times$  S.D. of the PBS alone group as positive.

## 2.9. In vivo cytotoxic T lymphocyte (CTL) assay

*In vivo* CTL assay was carried out as previously described [23]. C57BL/6 mice were dosed with OVA-NPs (small or large, 50  $\mu$ g of OVA per mouse,  $n = 4$ ) or sterile PBS ( $n = 3$ ) on days 0, 7, and 14. On day 21, splenocytes from naive C57BL/6 mice were pulsed with 0.2  $\mu$ M SIINFEKL peptide (GenScript) and labeled with 10  $\mu$ M of CFSE (CFSE<sup>High</sup>). Similarly, splenocytes that were not pulsed with SIINFEKL were labeled with a lower concentration of CFSE (1  $\mu$ M, CFSE<sup>Low</sup>). Ten million cells in each population were mixed and injected intravenously via the tail vein into the immunized mice. Mice were euthanized 16 h later, and the relative abundance of CFSE<sup>High</sup> and CFSE<sup>Low</sup> in their splenocyte preparation was determined using a flow cytometer (BD FACSCalibur Flow Cytometer, BD Biosciences, San Jose, CA). Specific lysis was calculated according to the following formula:  $(1 - (\text{ratio of CFSE}^{\text{low}}/\text{CFSE}^{\text{high}}$  of mice dosed with sterile PBS) / (ratio of CFSE<sup>low</sup>/CFSE<sup>high</sup> of mice dosed with the OVA-NPs))  $\times 100$ .

## 2.10. Uptake of the OVA-NPs by DC2.4 cells and J774A.1 cells in culture

Nanoparticles were labeled with fluorescein directly by incorporating DOPE-fluorescein (5%, w/w) prior to the conjugation of the OVA to generate fluorescein-labeled small or large OVA-NPs (OVA-NPs-fluorescein) [3]. DC2.4 cells or J774A.1 cells (50,000 cells/well) were seeded into 24-well plates and allowed to grow overnight at 37°C under 5% CO<sub>2</sub>. OVA-NPs-fluorescein (small or large, 50  $\mu$ l) were added into cells and incubated for 6 h at 37°C under 5% CO<sub>2</sub> or at 4°C. The cells were washed three times with PBS (10 mM, pH 7.4), lysed with Triton X-100 (Sigma, 0.5%, v/v), and incubate at -80°C for 1 h. Cells were then analyzed for fluorescence intensity using a BioTek Synergy HT Multi-Mode Microplate Reader (Winooski, VT). Data were presented as the percentage of fluorescein-labeled OVA-NPs internalized, which was calculated by subtracting the fluorescence intensity values obtained at 4°C from that obtained at 37°C and then normalized to the total amount of fluorescein-labeled nanoparticles added (fluorescence intensity).

## 2.11. Fluorescence microscopy

Small and large OVA-nanoparticles were labeled with fluorescein directly by incorporating DOPE-fluorescein (5%, w/w) before conjugating with OVA [3]. DC2.4 cells ( $2 \times 10^6$ ) were plated on poly-D-lysine-coated glass cover-slips overnight. Fluorescein-labeled OVA-nanoparticles were added into cells and incubated for 1 h at 37°C. After incubation, cells were washed with warm PBS and fixed with 3% paraformaldehyde for 20 min at room temperature. After washing with PBS three times, the cover-slips were mounted on slides using Vectashield mounting medium with DAPI. Fluorescent images were obtained using an Olympus BX60 Biological Microscope (Olympus America, Inc. Center Valley, PA).

## 2.12. Expression of MHC I/II and CD80 molecules on DC2.4 cells

DC2.4 cells were seeded into 6-well plates (50,000 cells/well) and allowed to grow overnight at 37°C under 5% CO<sub>2</sub>. The cells were then incubated with 75  $\mu$ l of OVA-free nanoparticles (small or large) or OVA in solution (5  $\mu$ g OVA) for 18 h at 37°C under 5% CO<sub>2</sub>. As controls, cells were treated with sterile PBS or lipopolysaccharides from *E. coli* (LPS, Sigma, 200 ng). The cells were washed with cold staining buffer (1% FBS and 0.1% NaN<sub>3</sub> in PBS), stained with anti-CD80, anti-I-A[b] MHC II, or anti-H-2Kb MHC I Ab for 20 min at 4°C, washed with staining buffer twice, and then analyzed with a BD

FACSCalibur flow cytometer or a Guava EasyCyte 8HT Microcapillary flow cytometer (Millipore Corporation, Hayward, CA). This experiment was repeated 2 more times with similar results. Finally, DC2.4 cells were also incubated with increased doses of nanoparticles (150 and 225  $\mu$ l) to evaluate the effect of the dose of the nanoparticles on the expression of MHC I, MHC II, and CD80.

### 2.13. In vivo uptake of nanoparticles by lymph node cells

Twenty-five  $\mu$ l of OVA-NPs-fluorescein (small or large) were subcutaneously injected into the footpad of one of the hind legs of mice ( $n = 5$ ). Sterile PBS (10 mM, pH 7.4) was injected as the negative control ( $n = 4$ ). Twenty-four h later, mice were euthanized, and the popliteal lymph node in the injected hind leg was removed and pooled to prepare a single cell suspension [24]. The cells were then analyzed using a Guava EasyCyte 8HT Microcapillary flow cytometer to estimate the percentage fluorescein positive lymph node cells [3]. This experiment was repeated one more time with similar results.

### 2.14. Statistical analysis

Statistical analyses were completed using ANOVA followed by Fischer's protected least significant difference procedure. Mouse survival curves were compared using the Kaplan–Meier survival analysis (GraphPad Prism, La Jolla, CA). A  $p$ -value of  $\leq 0.05$  (two-tail) was considered statistically significant.

## 3. Results and Discussion

### 3.1. Characterization of OVA-conjugated nanoparticles

Data shown in Table 1 are some of the properties of the OVA-nanoparticles. OVA-nanoparticles with a mean diameter of 230 nm and 708 nm were considered as small and large OVA-nanoparticles, respectively. The polydispersity indices of the large OVA-nanoparticles and the small OVA-nanoparticles were around 0.2 and 0.3, respectively. The micrographs of small and large OVA-nanoparticles are shown in Figure 1A. Overlaying of the dynamic light scattering spectra of the small and large OVA-nanoparticles revealed only a slight overlap (Figure 1B). The zeta potentials of the small and large OVA-nanoparticles were not different ( $p = 0.56$ ), and the amount of OVA conjugated onto the small and large nanoparticles were not different as well ( $p = 0.36$ ) (Table 1). Finally, the size and size distribution of the small and large OVA-nanoparticles did not change after 30 min of incubation at 37°C in normal saline or normal saline with 10% of FBS (data not shown), suggesting that the OVA-nanoparticles will not likely aggregate when injected into mice.

### 3.2. Nanoparticles showed potent adjuvant activity only when the antigen (OVA) was chemically conjugated onto their surface

Previously, it was shown that protein antigens (e.g., BSA or the protective antigen protein of *Bacillus anthracis*) conjugated onto the surface of the nanoparticles (around 200 nm) induced a strong, quick, long-lasting, and functional antibody response when subcutaneously injected into mice [3]. However, it remained unknown whether the protein antigens had to be covalently conjugated onto the surface of the nanoparticles for the nanoparticles to execute their adjuvant activity. To test this, the antibody responses induced by OVA chemically conjugated onto the nanoparticles (OVA-NPs) or physically mixed with the same nanoparticles (OVA+NPs) were evaluated. The nanoparticles used were the small nanoparticles as shown in Table 1. As expected, immunization of mice with OVA-conjugated nanoparticles induced a strong anti-OVA IgG response in mouse serum. However, immunization with the same amount of OVA physically mixed with the nanoparticles only induced a weak anti-OVA IgG response (Supplement S1). This is in

agreement with data from Fifis *et al.* [6] and Slutter *et al.* [25] who showed that the antigen of interest needed to be chemically linked with nanoparticles for the nanoparticles used in their studies to enhance the immune responses induced by the antigen [6]. The mechanism of immune stimulation by the nanoparticles is different from other immuno-stimulatory molecules such as CpG oligos and lipopolysaccharides, which do not have to be chemically conjugated to antigens to have adjuvant activity [26–27], although for the CpG oligos, conjugation of protein antigens with them helped further increase the resultant immune response [27]. Finally, it needs to be noted that one may not generalize that for all nanoparticle-based antigen carriers, protein antigens have to be covalently conjugated onto them for them to be immunostimulatory. For example, it was reported that protein antigens (e.g., cationized lactase, *Neisseria meningitidis* type B (MB), or HIV p55 Gag) simply mixed with anionic nanoparticles were strongly immunogenic in mice [17,28–29]. Similarly, antigens may not need to be chemically conjugated onto nanoparticles prepared with ionic polyphosphazenes for the nanoparticles to enhance the resultant immune responses because of the intrinsic adjuvant activity of the ionic polyphosphazenes [30–31].

### 3.3. Small OVA-conjugated nanoparticles induced stronger OVA-specific antibody and CTL responses than the large OVA-conjugated nanoparticles

Data in Figure 2A showed that the anti-OVA IgG level in mice that received the small OVA-nanoparticles was higher than in mice that received the large OVA-nanoparticles ( $p = 0.04$  and  $0.02$  at 1,000- and 10,000-fold dilutions, respectively). Similar results (Figure 2B) were obtained from another study. The anti-OVA IgG titer in mice that were immunized with the small OVA-nanoparticles was significantly greater than in mice that were immunized with the large OVA-nanoparticles ( $p = 0.0015$ , OVA-NPs, S vs. OVA-NPs, L) (Figure 2B). Interestingly, the anti-OVA IgG titer in mice that received the mixture of small and large OVA-nanoparticles was in between the titers in mice that received the small or large OVA-nanoparticles (Figure 2B). IgG isotype studies revealed high levels of IgG1, but no significant level of IgG2a, in the sera of mice that received the small or large OVA-nanoparticles (data not shown). The IgG1-biased antibody responses suggested that a Th2-biased response was induced by the OVA-nanoparticles. This is in agreement with data from a recent study by Jain *et al.* (2010), who showed that the specific IgG induced by another lipid-based nanoparticle surface-conjugated with OVA ( $81.8 \pm 1.0$  nm) was predominately IgG1 [32]. Interestingly, Mottram *et al.* (2007) showed that OVA conjugated onto 40–50 nm polystyrene beads induced strong Th1 responses as indicated by the high level of IFN- $\gamma$  secretion, but not IL-4, by splenocytes isolated from the immunized mice [13]. The same group previously reported that the size of OVA-conjugated beads was 232 nm [6, 9]. Differences in materials used to prepare the nanoparticles and routes of administration may have contributed to the different results. Mottram *et al.* (2007) injected their polystyrene-based nanoparticles intradermally to the hind footpads of mice ( $50 \mu\text{l}$  per footpad) [13]. Finally, data in Figure 2C showed that the large OVA-nanoparticles failed to induce a significant OVA-specific CTL response, but an OVA-specific CTL activity ( $21.1 \pm 2.3\%$ ) was detected in mice that received the small OVA-nanoparticles ( $p = 0.0003$ , OVA-NPs, S vs. PBS), clearly demonstrating that the small OVA-nanoparticles were capable of inducing cellular immune responses.

### 3.4. Treatment with small OVA-conjugated nanoparticles more effectively inhibited the growth of B16-OVA tumors in mice

To understand whether the small OVA-nanoparticles can induce a stronger anti-tumor activity than the large OVA-nanoparticles, mice with pre-established B16-OVA tumors were treated with small or large OVA-nanoparticles or the mixture of small and large OVA-nanoparticles. As shown in Figure 3A, treatment with the small OVA-nanoparticles more effectively inhibited the growth of the B16-OVA tumors than with the large OVA-

nanoparticles. The anti-tumor activity induced by the mixture of small and large OVA-nanoparticles was weaker than that induced by the small OVA-nanoparticles but stronger than that induced by the large OVA-nanoparticles. In another study, B16-OVA-bearing mice were treated with the small OVA-nanoparticles 7 days (instead of 4 days) after the tumor injection. Data in Figure 3B showed that treatment with the small OVA-nanoparticles significantly improved the survival of the B16-OVA-bearing mice ( $p = 0.011$ , PBS vs. OVA-NPs, S). Therefore, it appears that the small OVA-nanoparticles induced a strong anti-tumor activity, but more experiments need to be carried out to identify the extent to which the anti-tumor activity observed was CTL-mediated.

Taken together, it appears that the small OVA-nanoparticles induced stronger OVA-specific antibody and CTL responses than the large OVA-nanoparticles. The small and large OVA-nanoparticles were prepared with the same materials. Their zeta potentials were not different from each other (Table 1). Moreover, because the amounts of OVA conjugated onto 1 mg of small nanoparticles or 1 mg of large nanoparticles were not statistically different, mice that received the small or large OVA-nanoparticles should have received the same amount of OVA-free nanoparticles. Therefore, the difference in the immune responses induced by the small and large OVA-nanoparticles was very likely due to their difference in particle size. Finally, both small and large OVA-nanoparticles did not aggregate when incubated at 37°C in simulated biological media, suggesting that they did not aggregate at the injection site after subcutaneous injection. To illustrate how nanoparticle aggregation after injection can significantly affect the resultant immune responses, we mixed the small OVA-nanoparticles with an equal volume of BD Matrigel™, which flows freely at 4°C or on ice, but gels at body temperature. Immunization of mice with the OVA-nanoparticles in Matrigel™ induced a significantly weaker anti-OVA antibody response than with OVA-nanoparticles in sterile PBS (Supplement S2). Although more experiments will have to be carried out to understand why the OVA-nanoparticles in Matrigel™ were only weakly immunogenic, it is speculated that the gelling of the Matrigel™ at the injection site had significantly limited the interaction of the OVA-nanoparticles with APCs.

As mentioned earlier, there were a few previous reports that compared the immune responses induced by nanoparticle (diameter < 1000 nm)-based vaccine candidates, and the results from different studies were not in agreement [6–8]. Data from many previous studies indicated that the size of the nanoparticles also affected the type of immune responses induced [10,15]. It is interesting to find that both antibody and cellular responses induced by the small OVA-nanoparticles were stronger than that induced by the larger nanoparticles (Figure 2). The study by Fifis *et al.* (2004) was most relevant to the present study, in which the authors chemically conjugated OVA onto the surface of polystyrene particles of different size (20, 40, 100, 500, 1000, and 2000 nm) and reported that OVA conjugated onto the 40 nm nanoparticles induced the strongest antibody and cellular immune responses when given intradermally to mice [6]. In a later report, it was shown that the OVA/40-nm polystyrene nanoparticles had an average diameter of 230 nm, and the sizes of the other particles after conjugation with OVA were not reported [9]. Nonetheless, our data showed that by the subcutaneous route and when antigens were conjugated onto the surface of nanoparticles engineered from lecithin/GMS-in-water emulsions, small nanoparticles with a diameter of around 230 nm as a protein antigen carrier showed a more potent adjuvant activity than large nanoparticles of around 700 nm. The following studies were carried out to preliminarily elucidate the mechanisms responsible for the more potent adjuvant activity of the smaller 230 nm OVA-nanoparticles.

### 3.5. Small OVA-nanoparticles were more efficiently internalized by DCs and macrophages than large OVA-nanoparticles

Data from a previous study showed that the potent adjuvant activity of the small OVA-nanoparticles was likely due to their ability to move the antigens into local draining lymph nodes, to enhance the uptake of the antigens by APCs, and to activate APCs [3]. To preliminarily elucidate the mechanism(s) responsible for the more potent adjuvant activity from the small nanoparticles than the large nanoparticles, experiments were carried out to evaluate i) the extent to which APCs such as DCs and macrophage can take up the small and large nanoparticles in culture, ii) the extent to which the large and small nanoparticles regulate the expression of MHC I/II and CD80/86 molecules on DCs, and iii) the drainage of nanoparticles to local draining lymph nodes after subcutaneous injection.

To evaluate the extent to which APCs can take up the small and large nanoparticles, the uptake of the small and large OVA-nanoparticles by DC2.4 cells and J774A.1 macrophages in culture were measured. As shown in Figure 4A, after 6 h of incubation with DC2.4 cells or J774A.1 cells, more small OVA-nanoparticles than large OVA-nanoparticles were internalized by the cells. It seemed that the large OVA-nanoparticles just bound on the surface of the cells without being internalized. For example, as shown in Figure 4B, the % of large OVA-nanoparticles associated with the J774A.1 cells were not different regardless whether the nanoparticles and the cells were co-incubated at 37°C with 5% CO<sub>2</sub> or 4°C. In contrast, when the small OVA-nanoparticles were co-incubated with the J774A.1 cells for 6 h, much more particles were associated with the cells when the incubation was carried out at 37°C, 5% CO<sub>2</sub> than at 4°C (Figure 4B). The fluorescence micrographs shown in Figure 4C were also supportive of these findings. While the small OVA-nanoparticles were internalized and visible within the DC2.4 cells, the fluorescence from the large OVA-nanoparticles were concentrated only on the surface of the DC2.4 cells (Figure 4C). Similar findings have been reported by others [10, 18]. For example, Foged *et al.* (2005) showed that in culture, human DCs more readily took up particles smaller than 500 nm [18]. Kanchan and Panda (2007) showed that after *in vitro* incubation with mouse macrophage cells, 400 nm particles were internalized into the macrophages, whereas larger 2–8 µm particles were simply attached onto the surface of the macrophages [10].

### 3.6. Small and large nanoparticles had slightly different effects on the expression of MHC I/II and CD80 molecules on DC2.4 cells

To understand whether the small and large nanoparticles may exert different effects on the expression of DC maturation markers such as MHC I/II and CD80/CD86 molecules on APCs, the expression of the molecules on mouse DC2.4 cells was measured after stimulation with the small or large OVA-free nanoparticles. As shown in Figure 5A, the small nanoparticles slightly more effectively up-regulated the expression of CD80 and possibly MHC I molecules than the large nanoparticles, whereas the large nanoparticles slightly more effectively up-regulated the expression of MHC II molecules on the DC2.4 cells. CD86 expression on the DC2.4 cells was very high, and stimulation with the nanoparticles did not reveal any detectable changes in its expression (data not shown). Increasing the dose of the nanoparticles (2- or 3-fold) further enhanced the up-regulation of the CD80 on the DC2.4 cells, but it was more pronounced in cells incubated with the small nanoparticles than with the large nanoparticles (Fig. 5B). Similar, higher doses of nanoparticles led to more up-regulation of the MHC II on the DC2.4 cells, but it was more pronounced in cells incubated with the large nanoparticles (data not shown). For unknown reason, increasing the dose the nanoparticles did not lead to an enhanced up-regulation of the MHC I on DC2.4 (data not shown). The small and large OVA-free nanoparticles were prepared with the same materials, and thus, their differential effects on the expression of cell surface molecules were likely due to their particle size difference.

### 3.7. More small OVA-nanoparticles than large OVA-nanoparticles moved to local draining lymph nodes 24 h after injection

As shown in Figure 6, 24 h after subcutaneous injection into the footpad, more popliteal lymph node cells in mice that were injected with the small fluorescein-labeled OVA-nanoparticles were fluorescein positive than in mice injected with the large fluorescein-labeled OVA-nanoparticles, indicating that the small OVA-nanoparticles more efficiently drained to local lymph nodes than the large OVA-nanoparticles. This finding is in agreement with what was reported by Manolova *et al.* (2008), who showed that 24 h after injection, 500- and 1,000-nm polystyrene particles were barely detectable in mouse popliteal lymph nodes, whereas smaller particles of 20–200 nm were abundant in the popliteal lymph nodes [19]. Taken together, the more potent adjuvant activity from the small nanoparticles may be related to the following: i) APCs more effectively took up the small nanoparticles than the large nanoparticles; ii) The small nanoparticles more efficiently drained to local draining lymph nodes after injection; and iii) The small and large nanoparticles differed in their abilities to regulate the expression of MHC I/II molecules and the co-stimulatory CD80 molecule on APCs.

## 4. Conclusions

To our knowledge, this study represent the first study, in which all of the following nanoparticle formulation parameters were characterized before the antigen-loaded nanoparticles were dosed to animals to evaluate the resultant antibody and CTL immune responses: i) the particle size reported were measured after the antigens were loaded (conjugated) onto the particles; ii) the final antigen-loaded nanoparticles were relatively narrowly distributed, the different groups of nanoparticles did not extensively overlap; iii) the zeta potential of the two antigen-conjugated nanoparticles were not different; iv) the amount antigens loaded onto an unit weight (1 mg) of different nanoparticles were not different, and thus the amount of nanoparticles injected into the animals were the same for the two nanoparticles; v) the stability of the final antigen-loaded nanoparticles after dispersed into simulated biological media were evaluated prior to their injection into animals to make sure that the nanoparticles would not likely aggregate after injection. We then showed that by the subcutaneous route, the small 230 nm antigen-conjugated nanoparticles induced stronger antibody and cellular immune responses than the large 700 nm nanoparticles. Future efforts in using the lecithin/GMS-based nanoparticles or similar lipid-based nanoparticles with surface-conjugated antigens for vaccine development should use particles smaller than 500 nm, or preferentially around 200 nm, to generate strong antibody and cellular immune responses. Moreover, future efforts to correlate size of nanoparticles and their adjuvant activities should control the nanoparticle formulation parameters to ensure that the particle size is truly the only parameter that varies.

## Supplementary Material

Refer to Web version on PubMed Central for supplementary material.

## Acknowledgments

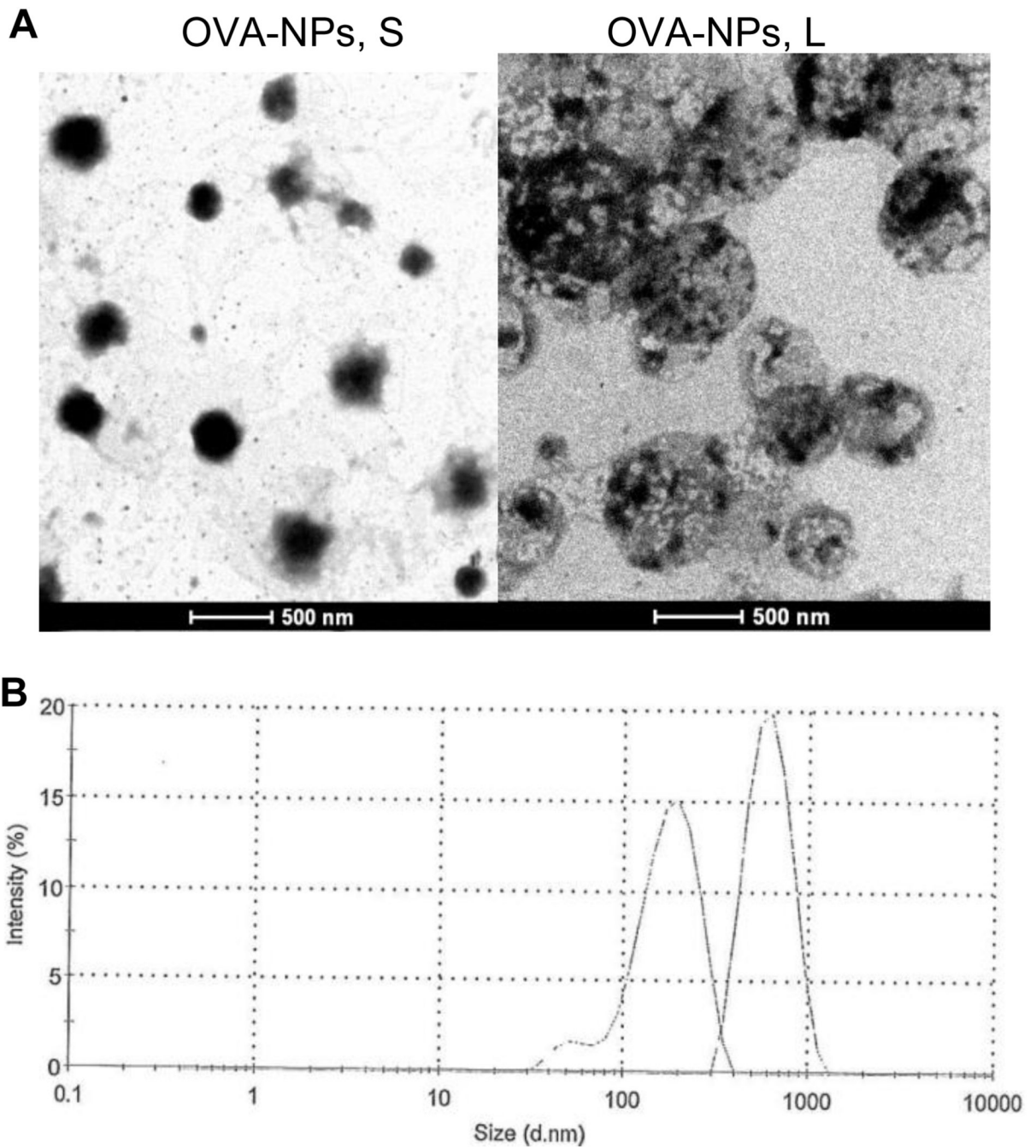
This work was supported in part by National Institute of Allergy and Infectious Diseases grants AI078304 and AI070538 to Z.C. N.Y. was supported in part by a fellowship from Payap University, Chiang Mai, Thailand.

## References

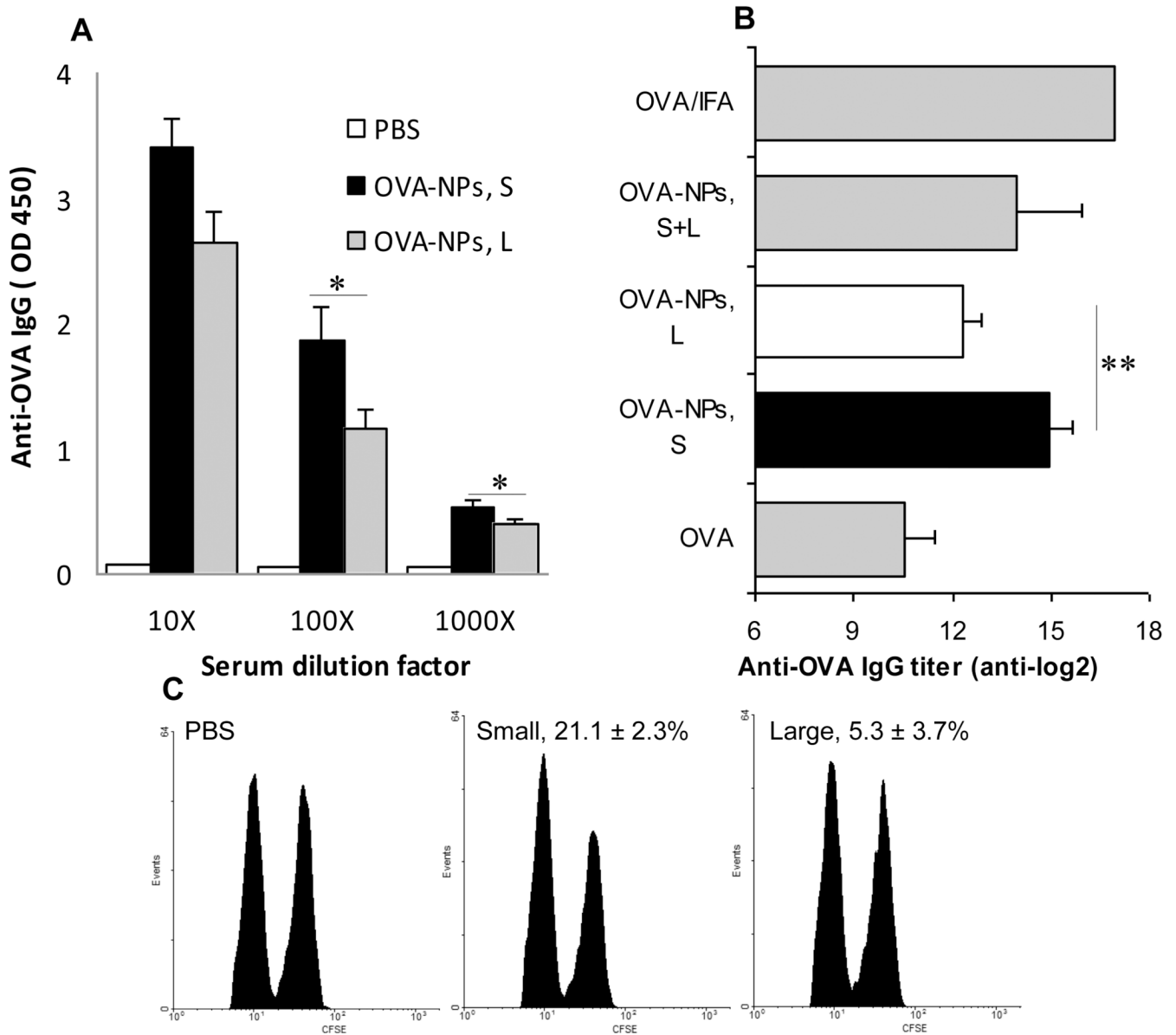
1. Cui Z, Mumper RJ. Microparticles and nanoparticles as delivery systems for DNA vaccines. *Crit Rev Ther Drug Carrier Syst.* 2003; 20:103–137. [PubMed: 14584521]

2. Peek LJ, Middaugh CR, Berklund C. Nanotechnology in vaccine delivery. *Adv Drug Deliv Rev.* 2008; 60:915–928. [PubMed: 18325628]
3. Sloat BR, Sandoval MA, Hau AM, He Y, Cui Z. Strong antibody responses induced by protein antigens conjugated onto the surface of lecithin-based nanoparticles. *J Control Release.* 2010; 141:93–100. [PubMed: 19729045]
4. Wendorf J, Singh M, Chesko J, Kazzaz J, Soewanan E, Ugozzoli M, O'Hagan D. A practical approach to the use of nanoparticles for vaccine delivery. *J Pharm Sci.* 2006; 95:2738–2750. [PubMed: 16927245]
5. Vila A, Sanchez A, Evora C, Soriano I, Vila Jato JL, Alonso MJ. PEG-PLA nanoparticles as carriers for nasal vaccine delivery. *J Aerosol Med.* 2004; 17:174–185. [PubMed: 15294069]
6. Fifis T, Gamvrellis A, Crimeen-Irwin B, Pietersz GA, Li J, Mottram PL, McKenzie IF, Plebanski M. Size-dependent immunogenicity: therapeutic and protective properties of nano-vaccines against tumors. *J Immunol.* 2004; 173:3148–3154. [PubMed: 15322175]
7. Gutierrez I, Hernandez RM, Igartua M, Gascon AR, Pedraz JL. Size dependent immune response after subcutaneous, oral and intranasal administration of BSA loaded nanospheres. *Vaccine.* 2002; 21:67–77. [PubMed: 12443664]
8. Jung T, Kamm W, Breitenbach A, Hungerer KD, Hundt E, Kissel T. Tetanus toxoid loaded nanoparticles from sulfobutylated poly(vinyl alcohol)-graft-poly(lactide-co-glycolide): evaluation of antibody response after oral and nasal application in mice. *Pharm Res.* 2001; 18:352–360. [PubMed: 11442276]
9. Kalkanidis M, Pietersz GA, Xiang SD, Mottram PL, Crimeen-Irwin B, Ardipradja K, Plebanski M. Methods for nano-particle based vaccine formulation and evaluation of their immunogenicity. *Methods.* 2006; 40:20–29. [PubMed: 16997710]
10. Kanchan V, Panda AK. Interactions of antigen-loaded polylactide particles with macrophages and their correlation with the immune response. *Biomaterials.* 2007; 28:5344–5357. [PubMed: 17825905]
11. Wendorf J, Chesko J, Kazzaz J, Ugozzoli M, Vajdy M, O'Hagan D, Singh M. A comparison of anionic nanoparticles and microparticles as vaccine delivery systems. *Hum Vaccin.* 2008; 4:44–49. [PubMed: 18438105]
12. Brewer JM, Tetley L, Richmond J, Liew FY, Alexander J. Lipid vesicle size determines the Th1 or Th2 response to entrapped antigen. *J Immunol.* 1998; 161:4000–4007. [PubMed: 9780169]
13. Mottram PL, Leong D, Crimeen-Irwin B, Gloster S, Xiang SD, Meanger J, Ghildyal R, Vardaxis N, Plebanski M. Type 1 and 2 immunity following vaccination is influenced by nanoparticle size: formulation of a model vaccine for respiratory syncytial virus. *Mol Pharm.* 2007; 4:73–84. [PubMed: 17274665]
14. Caputo A, Castaldello A, Brocca-Cofano E, Voltan R, Bortolazzi F, Altavilla G, Sparnacci K, Laus M, Tondelli L, Gavioli R, Ensoli B. Induction of humoral and enhanced cellular immune responses by novel core-shell nanosphere- and microsphere-based vaccine formulations following systemic and mucosal administration. *Vaccine.* 2009; 27:3605–3615. [PubMed: 19464541]
15. Mann JF, Shakir E, Carter KC, Mullen AB, Alexander J, Ferro VA. Lipid vesicle size of an oral influenza vaccine delivery vehicle influences the Th1/Th2 bias in the immune response and protection against infection. *Vaccine.* 2009; 27:3643–3649. [PubMed: 19464545]
16. Oyewumi MO, Kumar A, Cui Z. Nano-microparticles as immune adjuvants: correlating particle sizes and the resultant immune responses. *Expert Rev Vaccines.* 2010; 9:1095–1107. [PubMed: 20822351]
17. Cui Z, Mumper RJ. Coating of cationized protein on engineered nanoparticles results in enhanced immune responses. *Int J Pharm.* 2002; 238:229–239. [PubMed: 11996826]
18. Foged C, Brodin B, Frokjaer S, Sundblad A. Particle size and surface charge affect particle uptake by human dendritic cells in an in vitro model. *Int J Pharm.* 2005; 298:315–322. [PubMed: 15961266]
19. Manolova V, Flace A, Bauer M, Schwarz K, Saudan P, Bachmann MF. Nanoparticles target distinct dendritic cell populations according to their size. *Eur J Immunol.* 2008; 38:1404–1413. [PubMed: 18389478]

20. Brown DM, Fisher TL, Wei C, Frelinger JG, Lord EM. Tumours can act as adjuvants for humoral immunity. *Immunology*. 2001; 102:486–497. [PubMed: 11328383]
21. Shen Z, Reznikoff G, Dranoff G, Rock KL. Cloned dendritic cells can present exogenous antigens on both MHC class I and class II molecules. *J Immunol*. 1997; 158:2723–2730. [PubMed: 9058806]
22. Sloat BR, Sandoval MA, Cui Z. Towards preserving the immunogenicity of protein antigens carried by nanoparticles while avoiding the cold chain. *Int J Pharm*. 2010; 393:197–202. [PubMed: 20416366]
23. Cui Z, Qiu F. Synthetic double-stranded RNA poly(I:C) as a potent peptide vaccine adjuvant: therapeutic activity against human cervical cancer in a rodent model. *Cancer Immunol Immunother*. 2006; 55:1267–1279. [PubMed: 16362407]
24. Cui ZR, Han SJ, Vangasseri DP, Huang L. Immunostimulation mechanism of LPD nanoparticle as a vaccine carrier. *Mol Pharmaceut*. 2005; 2:22–28.
25. Slutter B, Soema PC, Ding Z, Verheul R, Hennink W, Jiskoot W. Conjugation of ovalbumin to trimethyl chitosan improves immunogenicity of the antigen. *J Control Release*. 2010; 143:207–214. [PubMed: 20074597]
26. Maurer T, Heit A, Hochrein H, Ampenberger F, O'Keeffe M, Bauer S, Lipford GB, Vabulas RM, Wagner H. CpG-DNA aided cross-presentation of soluble antigens by dendritic cells. *Eur J Immunol*. 2002; 32:2356–2364. [PubMed: 12209649]
27. Chikh G, de Jong SD, Sekirov L, Raney SG, Kazem M, Wilson KD, Cullis PR, Dutz JP, Tam YK. Synthetic methylated CpG ODNs are potent in vivo adjuvants when delivered in liposomal nanoparticles. *Int Immunol*. 2009; 21:757–767. [PubMed: 19502586]
28. Kazzaz J, Neidleman J, Singh M, Ott G, O'Hagan DT. Novel anionic microparticles are a potent adjuvant for the induction of cytotoxic T lymphocytes against recombinant p53 gag from HIV-1. *J Control Release*. 2000; 67:347–356. [PubMed: 10825566]
29. Singh M, Kazzaz J, Chesko J, Soenawan E, Ugozzoli M, Giuliani M, Pizza M, Rappouli R, O'Hagan DT. Anionic microparticles are a potent delivery system for recombinant antigens from *Neisseria meningitidis* serotype B. *J Pharm Sci*. 2004; 93:273–282. [PubMed: 14705185]
30. Andrianov AK, Marin A, Roberts BE. Polyphosphazene polyelectrolytes: a link between the formation of noncovalent complexes with antigenic proteins and immunostimulating activity. *Biomacromolecules*. 2005; 6:1375–1379. [PubMed: 15877355]
31. Mutwiri G, Benjamin P, Soita H, Babiuk LA. Co-administration of polyphosphazenes with CpG oligodeoxynucleotides strongly enhances immune responses in mice immunized with Hepatitis B virus surface antigen. *Vaccine*. 2008; 26:2680–2688. [PubMed: 18430493]
32. Jain A, Yan W, Miller KR, O'Carra R, Woodward JG, Mumper RJ. Tressyl-based conjugation of protein antigen to lipid nanoparticles increases antigen immunogenicity. *Int J Pharm*. 2010; 401:87–92. [PubMed: 20837122]



**Figure 1.** (A) Micrographs of OVA-nanoparticles. (B) Overlaying of the dynamic light scattering spectra of typical small and large OVA-nanoparticles. Left peak: OVA-NPs, S; Right peak: OVA-NPs, L.

**Figure 2.**

Small OVA-NPs induced stronger OVA-specific antibody and CTL responses than large OVA-NPs. **(A)** Mice ( $n = 7$ ) were dosed with small (OVA-NPs, S) or large OVA-NPs (OVA-NPs, L) on days 0, 7, and 14. Anti-OVA IgG level was measured on day 21 ( $n = 7$ ). \*,  $p < 0.05$ , OVA-NPs, S vs. OVA-NPs, L. **(B)** Mice ( $n = 3-5$ ) were dosed with small or large OVA-NPs or the mixture of them. As controls, mice were dosed with sterile PBS, OVA in PBS, or OVA/IFA. \*\*,  $p = 0.0015$  OVA-NPs, S vs. OVA-NPs, L. **(C)** OVA-specific CTL activity. Numbers are % cell lytic activity ( $p = 0.0003$ , OVA-NPs, S vs. OVA-NPs, L). The values of the OVA-NPs, L and the PBS groups were not different. Data shown are mean  $\pm$  S.D. ( $n = 4, 3$  for the PBS group).

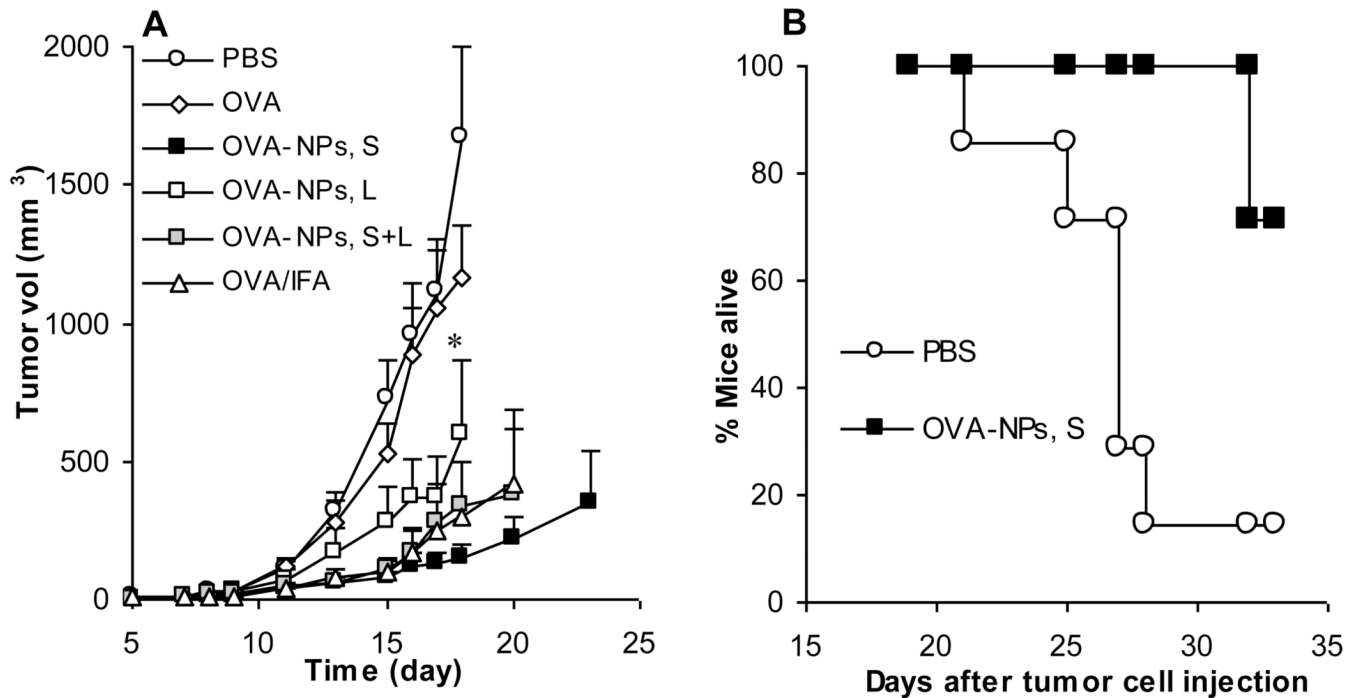


**Figure 3.**

Small OVA-NPs more effectively inhibited the growth of B16-OVA tumors in mice. **(A)** Mice ( $n = 7$ ) were s.c. injected with B16-OVA tumor cells on day 0. On days 4, 11, and 18, they were dosed with small OVA-NPs, large OVA-NPs, or the mixture of them. As controls, mice were dosed with sterile PBS, OVA in PBS, or OVA/IFA. Data shown are mean  $\pm$  S.D. \* On day 18,  $p = 0.03$ , OVA-NPs, S vs. OVA-NPs, L. **(B)** Mice ( $n = 6-7$ ) were subcutaneously implanted with B16-OVA tumor cells on day 0 and treated with small OVA-NPs on days 7, 14, and 21. Reported are days taken for tumors to reach 15 mm in diameter ( $p = 0.011$ , OVA-NPs, S vs. PBS).

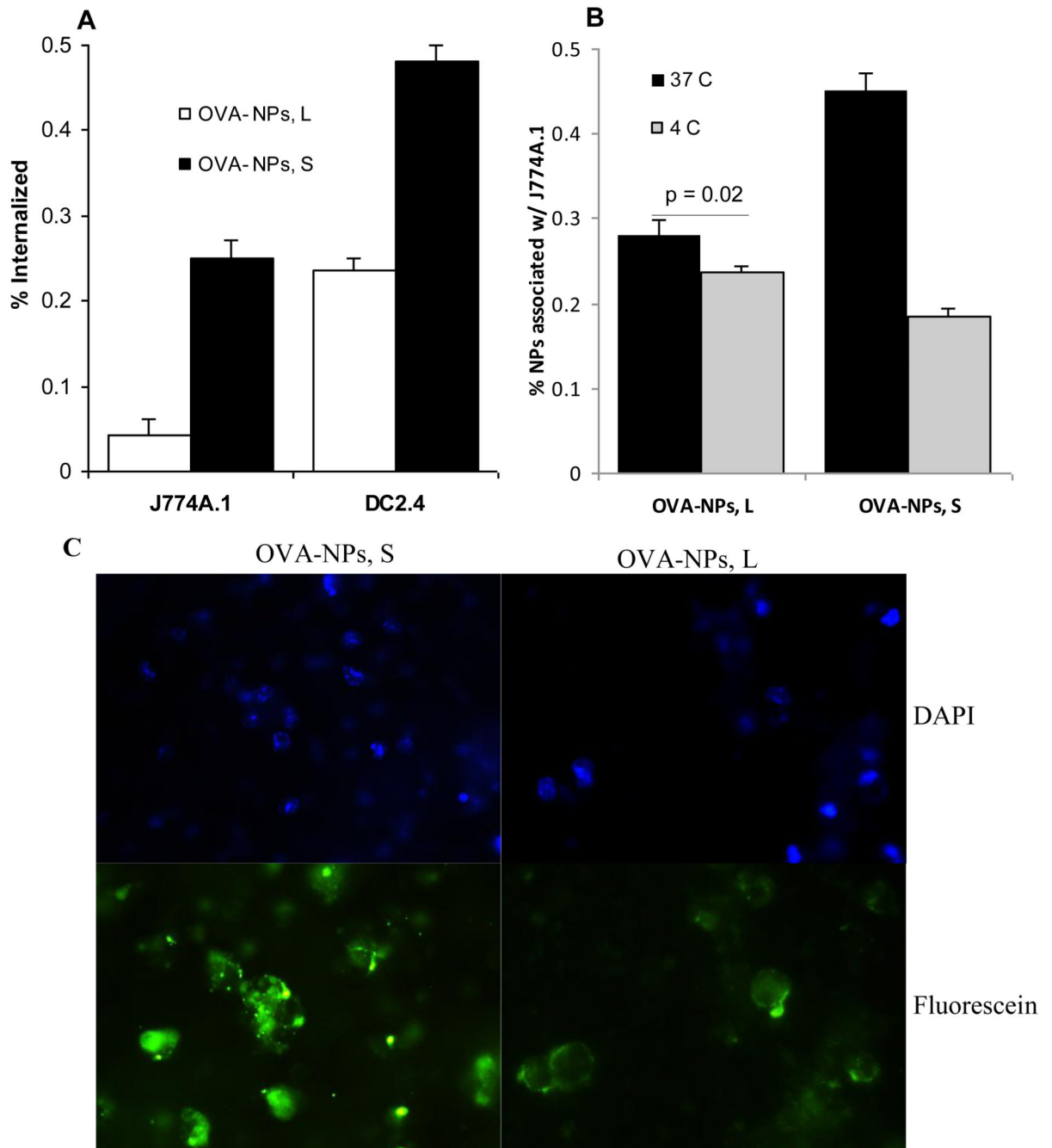


**Figure 4.**

In culture, small OVA-NPs were more efficiently internalized by DCs and macrophages than large OVA-NPs. Fluorescein-labeled OVA-NPs, large or small, were incubated with J774A.1 cells or DC2.4 cells for 6 h at 37°C with 5% of CO<sub>2</sub> or at 4°C. **(A)** % of nanoparticles internalized by J774A.1 or DC2.4 cells. **(B)** % of OVA-NPs associated (binding plus internalization) with J774A.1 cells after 6 h of incubation at 37°C or 4°C. Data reported are mean ± S.D. (n = 3). In **(A)**, p = 0.0006 in J774A.1 cells, p = 0.0004 in DC2.4 cells. In **(B)**, p < 0.001 for OVA-NPs, S. **(C)**. Fluorescence micrographs (40 x) of DC2.4 cells after incubation with fluorescein-labeled small or large OVA-NPs for 6 h. Upper: DAPI; Lower: Fluorescein; Left: OVA-NPs, S; Right: OVA-NPs, L.

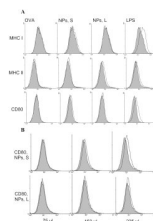


**Figure 5.**

Expression of MHC I/II and CD80 molecules on DC2.4 cells in culture after stimulation with OVA, small or large NPs, or LPS. **(A)**. DC2.4 cells were incubated with OVA, small or large OVA-free NPs, or LPS for 18 h before stained with Abs against CD80, I-A<sup>b</sup>, or 2-K<sup>b</sup>. Experiments were repeated 2–3 times with similar results. **(B)**. The effect of the dose of the nanoparticles (75, 150, and 225 μl), small or large, on the expression of CD80 on the DC2.4 cells.

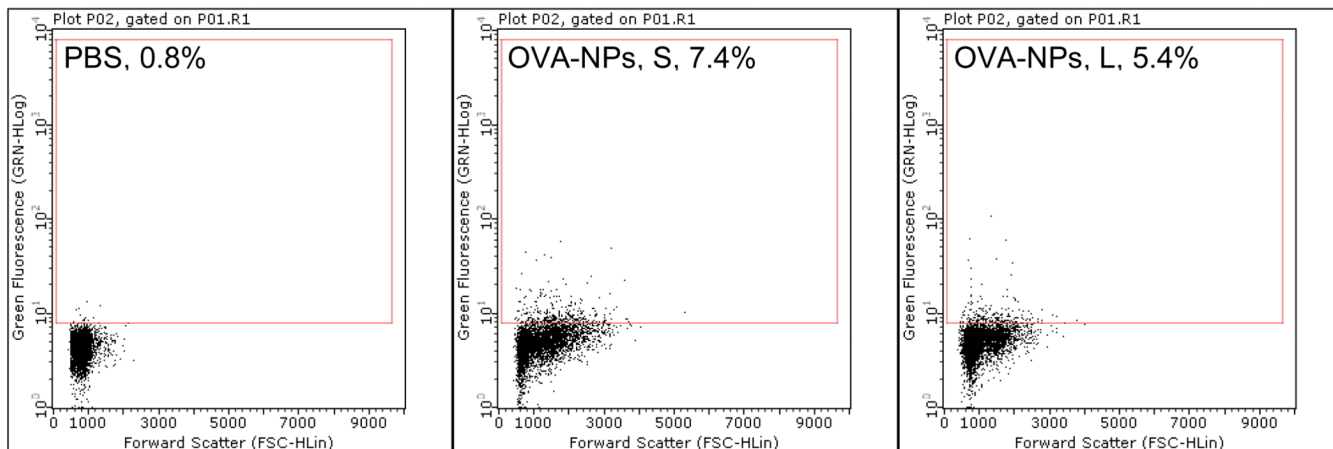


**Figure 6.**

More draining lymph node cells became fluorescein positive after subcutaneous injection of fluorescein-labeled small OVA-NPs than fluorescein-labeled large OVA-NPs. Fluorescein-labeled small or large OVA-NPs were injected into one hind leg footpad of mice. Popliteal lymph nodes were collected 24 h later, and single cell suspension was analyzed to determine the percentage of fluorescein<sup>+</sup> cells (number shown in gated area). Experiment was repeated once with similar result.

**Table 1**

**Nanoparticles before and after conjugation with OVA.** Data reported are mean  $\pm$  SD.

	Diameter of NPs (nm)		Zeta potential of OVA-NPs (mV)	[OVA] ( $\mu$ g/mg of NPs)
	NPs (n = 6)	OVA-NPs (n = 3)	(n = 3)	(n = 6)
Small nanoparticles	211 $\pm$ 20	230 $\pm$ 22	-30.5 $\pm$ 1.1 <sup>a</sup>	96.6 $\pm$ 11.0 <sup>b</sup>
Large nanoparticles	676 $\pm$ 32	708 $\pm$ 29	-30.8 $\pm$ 0.2 <sup>a</sup>	89.0 $\pm$ 16.1 <sup>b</sup>

Small OVA-NPs vs. large OVA-NPs,

<sup>a</sup> p = 0.56,

<sup>b</sup> p = 0.36.